HHS Public Access

Author manuscript

Free Radic Biol Med. Author manuscript; available in PMC 2018 February 20.

Published in final edited form as:

Free Radic Biol Med. 2011 May 15; 50(10): 1288–1296. doi:10.1016/j.freeradbiomed.2011.02.023.

ECSOD ALLELE-SPECIFIC EFFECTS ON ASBESTOS-INDUCED FIBROPROLIFERATIVE LUNG DISEASE IN MICE

Sujung Jun[1], **Cheryl L. Fattman**[2], **Byung-Jin Kim**[1], **Harlan Jones**[1], and **Ladislav Dory**[1,3]

[1]Department of Molecular Biology and Immunology, University of North Texas Health Sciences Center at Fort Worth, Fort Worth, TX 76107

[2]Department of Environmental and Occupational Health, University of Pittsburgh Graduate School of Public Health, Pittsburgh, PA 15219

Abstract

Previous work by others suggests that there is a strain-dependent variation in the susceptibility to inflammatory lung injury in mice. Specifically, the 129J mice appear to be more resistant to asbestos-induced pulmonary fibrosis than the C57BL/6 strain. A separate line of evidence suggests that extracellular superoxide dismutase (ecSOD) may play an important role in protecting the lung from such injuries. We have recently reported that the 129J strain of mice has an ecSOD genotype and phenotype distinctly different from those of the C57BL/6 mice. In order to identify ecSOD as a potential "asbestos-injury resistance" gene, we bred congenic mice, on the C57BL/6 background, carrying the wild type (*sod3*^{wt}) or the 129J (*sod3*^{129}) allele for ecSOD. This allowed us to examine the role of ecSOD polymorphisms in susceptibility to lung injury in an otherwise identical genetic background. Interestingly, asbestos treatment induces a significant (~40%) increase in plasma ecSOD activity in the *sod3*^{129} mice, but not in the *sod3*^{wt} mice. Asbestos administration results in a loss of ecSOD activity and protein from lung tissue of both congenic strains, but the lung ecSOD activity remains significantly higher in *sod3*^{129} mice. As expected, asbestos treatment results in a significant recovery of ecSOD protein in bronchoalveolar lavage fluid (BALF). The BALF of *sod3*^{129} mice also have significantly lower levels of proteins and inflammatory cells, especially neutrophils, accompanied by a significantly lower extent of lung injury, as measured by a pathology index score or hydroxyproline content. Immunohistochemistry reveals a significant loss of ecSOD from the tips of the respiratory epithelial cells in response to asbestos treatment and that the loss of immunodetectable ecSOD is compensated for by enzyme expression by infiltrating cells, especially in the *sod3*^{wt} mice. Our studies thus identify ecSOD as an important anti-inflammatory gene, responsible for most if not all of the resistance to asbestos-induced lung injury reported for the 129 strain of mice. The data further suggest allele-specific differences in the regulation of ecSOD expression. These congenic mice therefore represent a very useful model to study the role of this enzyme in all inflammatory diseases. Polymorphisms in human ecSOD have also been reported and it appears logical to assume that such variations may have a profound effect on disease susceptibility.

[3]To whom correspondence should be addressed to: UNT Health Science Center at Fort Worth, Department of Molecular Biology & Immunology, 3500 Camp Bowie Blvd., Fort Worth, TX 76107, Ph: 817-735-0180, Fax: 817-735-2118, Ladislav.Dory@unthsc.edu.

INTRODUCTION

Inhalation of asbestos fibers has long been known to cause asbestosis, pleural diseases, lung cancer, malignant mesothelioma and other cancers [1–3]. Asbestosis, a form of interstitial lung disease and one of the most frequent diseases caused by asbestos exposure, is characterized by inflammation and tissue fibrosis. It is a chronic, debilitating disease that leads to significant morbidity and mortality [2]. Although occupational exposures to asbestos fibers has decreased in recent years, the 20 to 40 year delay from exposure to manifestation of disease has resulted in increased incidence of asbestosis in exposed populations [1, 4, 5]. Thus, this disease currently is and will remain a significant health problem.

In the last 20 years, much work has been done to investigate both the pathogenesis and treatment of asbestos-related diseases. Nevertheless, many aspects remain poorly understood. A number of studies suggest that reactive oxygen species (ROS) -mediated inflammation and tissue damage contribute to the development and progression of interstitial pulmonary fibrosis (reviewed in [6, 7]). Previous studies have demonstrated that asbestos fibers, particularly of the amphibole class, can cause oxidative damage to the lung, primarily through the infiltration of the activated macrophages and neutrophils [8–10], although asbestos fibers can also directly generate ROS via reactive surface iron [11, 12]. In addition, over-expression of a number of antioxidant enzymes, including manganese superoxide dismutase and catalase [13, 14], as well as the addition of iron chelators [15] have been shown to be protective in a number of models of asbestos-induced lung disease.

The antioxidant enzyme extracellular superoxide dismutase (ecSOD) is the most abundant extracellular antioxidant in the lung [16–18]. This enzyme exists as a 135 kDa homotetramer composed of four 28 kDa subunits. ecSOD in the lung is bound to extracellular matrix (ECM) components through interaction with a positively charged heparin-binding domain located at the C-terminus of the enzyme (reviewed in [19]). Exposure of mice to a variety of injurious agents, including asbestos fibers, leads to the development of pulmonary fibrosis [7, 20, 21]. This is accompanied by loss of ecSOD from the alveolar septa and accumulation of the enzyme in the BALF [22, 23]. Evidence suggests that release of the enzyme may be mediated by proteolytic cleavage of the heparin-binding domain by proteases of neutrophil and macrophage origin [24, 25]. While it is not clear whether loss of ecSOD contributes to and/or is a result of the ongoing pathology, the former seems to be the case, as lung pathology is significantly exaggerated in ecSOD knockout mice [26, 27]. Recent studies indicate that inhibition of oxidative fragmentation of ECM probably represents one mechanism by which ecSOD inhibits inflammation in response to lung injury [28].

It has been reported that the 129P3/J (or 129J) mice are significantly more resistant to asbestos-induced pulmonary fibrosis than the C57BL/6 mice [29–31]. This phenotype is also associated with reduced expression of pro-fibrotic cytokines at sites of fiber deposition. Since the 129 strain of mice differs from the C57BL/6 strain in a number of other genes, finding the “susceptibility” gene(s) by a direct comparison of the two strains would be a difficult if not impossible task.

We [32] previously reported the existence of an allelic variant of ecSOD (*129*) found only in the 129P3/J strain of mice. Relative to the wild-type allele (*wt*), found in the C57BL/6 and other strains, this variant yields mRNA with a 10 bp deletion in the 3′ untranslated region (UTR) and several point mutations in the coding sequence. Two of the point mutations result in amino acid substitutions: one at the signal peptide cleavage site (N21D) and one within the catalytic region (A186S). This genotype has a profound effect on the ecSOD phenotype: both, plasma ecSOD levels and activities in the 129P3/J mice are 2-3 fold higher than those in the C57BL/6 mice suggesting no apparent change in specific activity. In order to investigate further the role of ecSOD as a "susceptibility" gene in asbestos-induced injury, we generated, by extensive crossbreeding and continuous genotyping, congenic mice expressing either the *129* or *wt* allele on a 99.9% C57BL/6 background (C57.129-*sod3*) [33]. The congenic mice that express the 129 allele ($sod3^{129}$) recapitulate the phenotypic differences in an allele-specific manner, in terms of free and heparin-releasable plasma ecSOD levels, activities, tissue enzyme distribution and relative tissue mRNA abundance [33]. These results suggest that most if not all of the observed ecSOD phenotype is allele-driven. This animal model enabled us to investigate specifically the role of ecSOD in an otherwise identical genetic environment.

We now present evidence that substituting the ecSOD allele from 129P3/J on the genetic background of a C57BL/6 mouse significantly changes the response of the animal to a fibrotic stimulus; specifically, the congenic $sod3^{129}$ mice are significantly protected against asbestos-induced inflammation and fibrotic lung disease relative to $sod3^{wt}$ mice. Our findings demonstrate that a single gene polymorphism can modulate disease susceptibility and highlight the significance of active ecSOD in the amelioration of asbestos-induced lung disease.

METHODS

Animals & asbestos exposure

8-10 weeks old female congenic $sod3^{wt}$ and $sod3^{129}$ mice, derived as previously described [33], were treated with 0.1 mg NIEHS crocidolite asbestos (> 10 μm in length) or 0.9% saline by intratracheal instillation, as previously described [23, 25]. Mice were euthanized at 14 days post-treatment. BALF was obtained by intratracheal instillation and recovery of 1 ml of 0.9% saline. Lungs were perfused with ice-cold PBS via cardiac puncture to remove residual blood. Lungs were removed and either flash-frozen in liquid nitrogen and stored at −80 °C until used for biochemical analysis or inflation-fixed with 10% formalin for histological analysis. All animals were treated by experimental protocols approved by the UNT HSC Institutional Animal Care and Use Committee.

ecSOD activity

Frozen lungs were ground to a fine powder in liquid nitrogen, and homogenized with 50 mM potassium phosphate buffer containing 0.3 M KBr and 3 mM EDTA, pH 7.4 containing a 1:1000 dilution of a protease inhibitor cocktail (100 μM 4-(2-aminoethyl) benzensulfonyl fluoride, 10 μM leupeptin, 10 μM E-64, 1 μM bestatin, 15 nM aprotinin, 1.0 μM pepstatin-A). The protein concentration of tissue homogenates was determined by Lowry assay [34].

ecSOD was partially purified using ConA Sepharose (Sigma) as described [35], using 2mg homogenate protein. Plasma aliquots (100 μL) were applied to ConA-Sepharose columns directly. The activity of ecSOD (released from ConA) was determined using an assay based on the oxidation of NAD(P)H [36]. Dismutase activity was estimated from a standard curve constructed by measuring the activity of increasing and known amounts of Cu/Zn SOD (Sigma, cat. #S2515). Activities are therefore expressed as ng of Cu/Zn SOD equivalents.

Western blots

Rabbit anti-mouse ecSOD antiserum was produced against a synthetic mouse-specific 21-amino acid peptide corresponding to the N-terminus of the mature protein, as previously described [32]. 20μL of diluted (1:40) plasma, 20μL aliquots of BALF or 10μg of lung homogenate protein were dissolved and boiled in Laemmli buffer containing 5% β-mercaptoethanol [37] for 5 min, separated by 12% SDS-PAGE at 100 V for 3.5 hours and transferred to polyvinylidine fluoride membranes (Bio-Rad) for 2 hours. After blocking in 5% milk TBST for 1 hour, the membranes were incubated with the primary antibody against ecSOD (1:20,000) and/or β-actin (1:5,000) rabbit anti-mouse antiserum (Sigma) overnight at 4 ˚C. Secondary antibodies (goat anti-rabbit IgG), conjugated to horseradish peroxidase (Jackson Immunoresearch) were added for 2 hours at RT (1:5,000 dilution). ecSOD and ß-actin bands were visualized by the ECL system (Amersham) using FluorChem® FC2 Imaging System (Alpha Innotech) and densitometric analysis was done using the software supplied (AlphaEaseFC) for the instrument. Transfer efficiency between runs was checked and corrected for by using aliquots of pooled mouse lung homogenates in each of the outside lanes. Moreover, scans were also corrected for loading by detecting ß-actin in lung samples.

Histological analysis

Five-micron thick lung sections from three levels (anterior, medial and posterior) were subjected to hematoxylin and eosin staining (Derm-Prep, FL, USA) and scored by Dr. Suarez (pathologist, Derm-Prep), blinded to sample groups. Individual fields were examined with a light microscope. Scoring in each level was based on the severity of bronchioles/alveolar tissue with interstitial fibrosis as well as inflammation according to the following scale: 0 = negative, 1 = minimal, 2 = moderate, 3 = moderate/severe, 4 = severe. Scores were calculated for each animal, and the group scores were averaged together for statistical comparisons.

Immunohistochemisty

Five-micron thick paraffin embedded medial lung sections were subjected to immunohistochemical staining with anti-ecSOD rabbit serum (1:1,000) or pre-immune rabbit serum (control). Sections were then labeled for ecSOD using an indirect immunoperoxidase method with a biotinylated goat anti-rabbit IgG and Biotin-horseradish peroxidase/Avidin (ABC staining kit from Vector Laboratories). To reduce background staining the sections were incubated in 0.3% H_20_2 in PBS to inactivate endogenous peroxidases, 0.05M glycine to block aldehydes, and nonspecific binding was blocked by incubation with 5% normal goat serum, 5% Avidin-Biotin solution (Blocking kit from Vector Laboratories). Staining was developed using the DAB kit (Vector Laboratories). Sections were counter-stained with hematoxylin (Vector Laboratories) followed by

dehydration and mounting. The sections were visualized with an Olympus AX70 upright microscope and an Olympus DP 70 Digital Camera for high-resolution imaging.

Analysis of BALF

Total protein in BALF was determined by Lowry assay [34]. Total cell counts in BALF were obtained using a Beckman Coulter Z1 particle counter (Beckman Coulter, Fullerton, CA). To obtain differential cell counts, total BALF cells were collected by spinning 1000×g at 4 °C for 10 min and sorted for cell type by flow cytometry.

Flow cytometry

Collected BALF cells were incubated with anti-CD16/CD32 FcRII/III blocker at 4 °C for 10 min. Multi-color immunofluorescence staining was performed using PE-labeled anti-mouse Ly6G (1A8), PE labeled anti-mouse SiglecF, PEcy7-labeled anti-mouse CD11b, alexafluo 488 (AF488)-labeled anti-mouse F4/80, APC-labeled anti-mouse CD19 and FITC-labeled anti-mouse B220 (CD45R) at 4 °C for 30 min. After washing twice, positive cells for immunostaining were identified using the Cytomic FC500 flow cytometry analyzer (Beckman–Coulter). Further analysis to determine proper cell population was performed using CXCP software (Beckman-Coulter). Anti-mouse antibodies for Ly6G, SiglecF, CD11b and B220 and Fc blocker were purchased from BD Biosciences (San Jose, CA). Anti-mouse antibodies for F4/80 and CD19 were purchased from Caltag® (InVitrogen Co. Carlsbad, CA).

Hydroxyproline assay

Whole lungs were dried and acid hydrolyzed in sealed oxygen-purged glass ampoules containing 2 ml of 6 N HCl for 24 h at 110 °C. Samples were centrifuged at 14,000 rpm and supernatant was taken for hydroxyproline analysis using chloramine-T, as previously described [38].

Statistical Analyses

Results from experiments are reported as means±SEM. All quantitative data are assessed for significance using either a Student's t-test or a one-way ANOVA with Tukey's post-hoc test (GraphPad Prism). A p value < 0.05 is used to establish significance.

RESULTS

The effect of asbestos treatment on plasma ecSOD levels

Although there is little doubt that that the asbestos-related lung pathogenesis is related to oxidative stress and the resulting inflammatory response, it has not been determined if such an oxidative stress can elicit systemic changes in ecSOD expression. We have therefore examined changes in plasma ecSOD protein levels and activities, as a result of asbestos treatment and the results are shown in Figure 1 A (protein levels) and B (activities). Saline-treated congenic $sod3^{129}$ mice express a significantly (2-fold) higher levels of ecSOD in the plasma, when compared to $sod3^{wt}$ mice. Interestingly, while asbestos treatment significantly

increases both, plasma ecSOD enzyme level and activity in *sod3*^{129} mice by 40%, it has no effect on ecSOD expression in the *sod3*^{wt} mice.

ecSOD protein levels, C-terminal processing and activity levels

To examine the effect of the 129 allele on distribution of ecSOD in the lung parenchyma and airspaces 14 days after asbestos treatment, Western blots were performed on lung homogenates and BALF. Saline-treated congenic *sod3*^{129} mice express a higher level of ecSOD in the lung, when compared to *sod3*^{wt} mice (Figure 2 A and 2 B). Asbestos treatment results in decreased ecSOD protein abundance in both groups of mice after 14 days, but the decrease in the *sod3*^{129} lung is significant, while the changes in *sod3*^{wt} lungs are insignificant (Figure 2 B). Following asbestos treatment both groups of mice have similar amount of ecSOD protein left in their lung tissues.

Asbestos-elicited changes in lung ecSOD enzyme level are accompanied by similar changes in ecSOD activities, as shown in Figure 2 C. In the control, saline-treated group lung ecSOD activities are higher in *sod3*^{129} mice than in *sod3*^{wt} mice. Asbestos treatment significantly reduces this activity in both groups, but significant differences in ecSOD activities remain: despite similar enzyme protein levels, ecSOD activity remains significantly higher in the *sod3*^{129} mice.

In agreement with previous reports [23, 25, 27], asbestos treatment results in a marked release of ecSOD into the BALF, regardless of the ecSOD genotype (Figure 2 D); the extent of asbestos-induced ecSOD protein release is similar in the two treatment groups.

As expected, the enzyme recovered from the BALF from both treatment groups is predominantly in the cleaved form, which lacks the heparin-binding domain (Figure 2 A and 2 E). In addition, the ratio of cleaved to uncleaved (full length) subunits of ecSOD increases in the lungs as well as BALF after asbestos-treatment, regardless of the ecSOD genotype (Figure 2 E).

Expression of lung ecSOD during asbestos-induced injury

We also examined asbestos-induced changes in ecSOD expression in the lungs of the congenic mice by immunocytochemsitry. In saline-treated mice, regardless of the ecSOD genotype, the most intense ecSOD staining appears to be in airways, including the lining of the bronchioli and the alveoli (Figure 3 A); increased magnifications of the respiratory epithelium of small bronchioli (as indicated by arrows) are shown in Figure 3 B. Intense ecSOD staining is apparent on the tips of the columnar epithelial cells of saline treated lungs; the staining is typically more intense in epithelial cells of *sod3*^{129} mice. The distinct, intense ecSOD staining of tissue derived from saline-treated lungs is replaced by a more diffuse, far less intense staining of tissues derived from asbestos-treated lungs, suggesting loss of enzyme. The ecSOD staining of the pneumocytes lining the alveoli and the alveolar ducts (areas devoid of cellular infiltration) appears to be more intense in both saline as well as asbestos-treated *sod3*^{129} mice, relative to the *sod3*^{wt} mice (Figure 3C). Immunohistochemistry does not demonstrate obvious differences in total ecSOD expression (staining) between the congenic groups, but clearly shows the abundant expression of this enzyme in areas infiltrated by immune cells. It should be also noted that the lungs of *sod3*^{wt}

mice have significantly more infiltrated areas, at the expense of alveolar areas, relative to the lungs of *sod3*^{129} mice (the lungs of *sod3*^{129} mice have significantly fewer such areas). Background staining using non-immune primary antiserum is shown in Figure 3 D and E.

Sod3^{129} mice exhibit reduced levels of acute lung injury markers

To evaluate the effect of the 129 allele on asbestos-induced lung injury, BALF from saline- or asbestos-treated *sod3*^{129} or *sod3*^{wt} mice was analyzed for markers of acute lung injury. The two groups of saline-treated mice do not differ in BALF protein or cell content (Figure 4 A and B). As expected, asbestos treatment results in a significant increase in both BALF markers isolated from asbestos-treated *sod3*^{129} or *sod3*^{wt} mice. However, both the amount of protein and the total number of inflammatory cells in BALF isolated from asbestos-treated *sod3*^{129} mice are significantly lower (~30% decrease) than those in BALF from *sod3*^{wt} mice (304.0±30.16 μg vs. 444.0±45.93 μg and 2.16±0.24 × 10^6 vs. 3.27±0.37 × 10^6 cells, respectively).

Flow cytometry reveals the presence of macrophages, B cells, neutrophils and eosinophils in the BALF of both groups of mice (Figure 5). There are no significant differences in the numbers of each cell type found in BALF of saline-treated mice of either ecSOD genotype. Macrophages are the dominant cell type in both groups of mice. Asbestos treatment induces a profound increase in eosinophils and neutrophils, and a marked reduction in macrophages. The relative increase in neutrophils and, to lesser extent eosinophils is markedly reduced in *sod3*^{129} mice. These results suggest a reduced inflammatory response to asbestos in the *sod3*^{129} lungs. In agreement with previous study [27], asbestos instillation reduces the macrophage content in BALF of both congenic mice (Figure 5 A).

Asbestos-induced lung fibrosis is reduced in sod3^{129} mice

To evaluate the effect of the 129 allele on asbestos-induced lung fibrosis, lungs from saline- or asbestos-treated mice were assessed for fibrosis. Analysis of lung tissue pathology from asbestos-treated *sod3*^{129} and *sod3*^{wt} mice indicates that both strains respond to the presence of asbestos fibers by mounting an inflammatory response that progresses into patchy, heterogeneous fibrotic lesions by 14 days post-treatment (Figure 6 A). A semi-quantitative assessment of lung tissue pathology, shown in Figure 6 B, indicates a significantly reduced (~20%) fibrosis in the *sod3*^{129} lungs (2.64 ± 0.21) relative to the *sod3*^{wt} mice (3.20 ± 0.18). Saline treatment does not lead to significant fibrosis in either group of mice.

The extent of fibrosis in the lungs of asbestos-treated animals was also evaluated by hydroxyproline levels - an index of collagen deposition. In agreement with the pathology index data, hydroxyproline levels are also significantly elevated in asbestos-treated animals relative to saline-treated controls (Figure 6 C). Moreover, the hydroxyproline level in asbestos-treated *sod3*^{129} mice (109.21 ± 4.46 μg / lung) is significantly lower when compared to that of the lungs of *sod3*^{wt} mice (124.0 ± 4.82 μg / lung).

DISCUSSION

Strain-specific differences in susceptibility to asbestos-induced injury have been previously reported. Brass *et al.* have shown that 129P3/J (or 129J) mice develop a reduced fibro-

proliferative response to inhaled asbestos, relative to 'fibrosis-sensitive' C57BL/6 mice [29]. They also showed that primary lung fibroblasts from the 129J mice proliferate more slowly, make less collagen, and have a reduced response to pro-fibrotic growth factors [30]. In addition, even with direct application of pro-fibrotic TGF-β to the lung parenchyma, the 129 mice have a reduced degree of disease and a delay in the development of fibrogenesis [31]. To-date there is little or no information regarding the genetic loci responsible for the observed differences between the strains.

In an independent line of research, studies have described a protective role for ecSOD in acute and fibrotic lung injuries [26]. An acute loss of this enzyme by a conditional knockout model using Cre-Lox technology leads to severe lung damage in the presence of ambient air [39]. A protective role for ecSOD is further supported by the fact that ecSOD KO mice are significantly more susceptible to injuries that cause pulmonary fibrosis, including asbestos exposure [26, 27, 40].

Given the strain-specific response to asbestos, the potential importance of ecSOD and our recent report that the 129 strain of mice express an allelic variant of ecSOD of a profoundly different phenotype, we decided to breed congenic mice, on the C57 background, which express either allele of ecSOD [33]. This experimental model enables us to examine the role of ecSOD specifically, independent of the genomic environment, in a number of inflammatory diseases.

Although we suspected that the increased expression of ecSOD in mice with the *129* allele may result in increased protection against asbestos-induced lung pathology, the additional increase in plasma ecSOD expression in these mice in response to the treatment was unexpected and not previously reported. Allele-specific differences in the regulation of expression of ecSOD have not been previously reported and may play a significant role in protection from oxidative stress. Our unpublished data suggest that the increased expression of ecSOD driven by the 129 allele is, at least partially, due to increased efficiency in signal peptide cleavage (the site of one of the amino acid substitutions) during enzyme synthesis. In addition to already higher levels of ecSOD in the $sod3^{129}$ mice, additional up-regulation of expression in the face of oxidative stress may further contribute to the protective effect of this allele for ecSOD; it may also be responsible for the diminished reduction in ecSOD activity observed in $sod3^{129}$ mice after asbestos treatment.

Our data indicate that, in agreement with others [41–43], increased levels of lung ecSOD in mice attenuate inflammation. The $sod3^{129}$ mice have significantly higher lung ecSOD activity even after asbestos treatment, potentially a function of higher starting amounts as well as differences in their response to asbestos-mediated oxidative stress. Analysis of the BALF as well as immunohistological analysis of the tissue suggests that the lack of significant change in ecSOD protein level of the $sod3^{wt}$ lungs is likely due to the compensatory acquisition of large amounts of "exogenous" ecSOD from the infiltrating inflammatory cells, as previously suggested by Tan *et al.* [25]. The inflammatory cell-derived enzyme may well be rapidly degraded/inactivated in the $sod3^{wt}$ strain, likely due to the oxidative stress. In terms of ecSOD protein amounts, our immunohistochemical data support this observation. Our results indicate that the recruited inflammatory cells are likely

the source of the majority of ecSOD expression in *sod3*^{wt} mice; decreased infiltration in the lungs of the *sod3*^{129} mice and thus decreased expression of inflammatory cell ecSOD appears to be compensated for by the increased ecSOD expression by lung epithelial and alveolar (type I pneumocytes) cells of the *sod3*^{129} mice.

Our data are also in accord with previous observations that ecSOD specifically inhibits neutrophil influx in response to asbestos [27]. Several studies have shown that ecSOD may inhibit pulmonary inflammation, specifically neutrophil chemotaxis, in part by preventing superoxide-mediated fragmentation of ECM components such as hyaluronan and syndecan-1 [28, 44, 45]. A similar mechanism is likely operating in our experiments: the increased initial activity of ecSOD in *sod3*^{129} lungs quenches the ROS induced by asbestos which, in turn, leads to a reduction in the oxidative fragmentations of ECM, decreased recruitment of neutrophils and decreased fibrosis.

Our results demonstrate that ecSOD is a prominent “fibrosis-resistance/anti-inflammatory” gene, responsible for the increased resistance of the 129 strain of mice to lung injury and fibrosis. We suggest that the increased initial ecSOD activity in the *sod3*^{129} mice, as well as the allele-specific up-regulation of ecSOD reduces the asbestos-induced oxidative stress and the resulting magnitude of inflammation. Indeed, expanding our observations to those of Fattman *et al.* [27], these studies cover a range of mice with high (*sod3*^{129}), intermediate (*sod3*^{wt}) and no (ecSOD KO) enzyme activity on an identical (C57BL/6) genetic background. It is clear that the extent of lung injury in response to asbestos is inversely proportional to lung ecSOD activity. Our recent studies demonstrate that the increased expression of the 129 form of ecSOD is allele-driven: the 129 ecSOD phenotype is observed even when immersed in the C57 genome [33].

Human ecSOD polymorphism is associated with a number of diseases, including COPD, ischemic heart disease, atherosclerosis and diabetes [46–51]. While protective against COPD, the R213G substitution is associated with increased risk of ischemic heart disease in heterozygotes [46, 49, 51]. The A40T polymorphism appears to be associated with susceptibility to Type 2 diabetes, and insulin resistance and hypertension [50]. Clearly, variations in ecSOD expression due to polymorphism may play a major role in the redox status of tissues, and thus disease susceptibility in humans.

In conclusion, ecSOD gene polymorphism clearly modulates susceptibility to asbestos-induced lung injury in mice. The congenic mice used in this study may provide an excellent model to examine the role of ecSOD in other diseases involving oxidative stress and an inflammatory response.

Acknowledgments

We thank Dr. Bhalchandra J. Kudchodkar for his helpful comments and critical reading of this manuscript. We are grateful to Ms. Alicia Benson and Mr. Pratikkumar Desai for their outstanding animal care.

This work was supported by grant from the National Institutes of Health (NHLBI) # RO1 HL70599.

References

1. Kamp DW, Weitzman SA. Asbestosis: Clinical spectrum and pathogenic mechanisms. Proc Soc Exp Biol Med. 1997; 214:12–26. [PubMed: 9012357]
2. Manning CB, Vallyathan V, Mossman BT. Diseases caused by asbestos: Mechanisms of injury and disease development. Int Immunopharmacol. 2002; 2:191–200. [PubMed: 11811924]
3. Kamp DW. Asbestos-induced lung diseases: An update. Transl Res. 2009; 153:143–152. [PubMed: 19304273]
4. Murphy RL Jr. The diagnosis of nonmalignant diseases related to asbestos. Am Rev Respir Dis. 1987; 136:1516–1517. [PubMed: 3688654]
5. Selikoff IJ, Hammond EC, Seidman H. Latency of asbestos disease among insulation workers in the united states and canada. Cancer. 1980; 46:2736–2740. [PubMed: 7448712]
6. Fattman, CL., Chu, CT., Oury, TD. Experimental models of asbestos-related diseases. In: Roggli, VL.Sporn, T., Oury, TD., editors. Pathology of Asbestos-Associated Diseases. 2nd. Little, Brown and Company; Boston: 2002.
7. Kinnula VL, Fattman CL, Tan RJ, Oury TD. Oxidative stress in pulmonary fibrosis: A possible role for redox modulatory therapy. Am J Respir Crit Care Med. 2005; 172:417–422. [PubMed: 15894605]
8. Dorger M, Allmeling AM, Kiefmann R, Munzing S, Messmer K, Krombach F. Early inflammatory response to asbestos exposure in rat and hamster lungs: Role of inducible nitric oxide synthase. Toxicol Appl Pharmacol. 2002; 181:93–105. [PubMed: 12051993]
9. Hansen K, Mossman BT. Generation of superoxide (O2-.) from alveolar macrophages exposed to asbestiform and nonfibrous particles. Cancer Res. 1987; 47:1681–1686. [PubMed: 3028612]
10. Rola-Pleszczynski M, Rivest D, Berardi M. Asbestos-induced chemiluminescence response of human polymorphonuclear leukocytes. Environ Res. 1984; 33:1–6. [PubMed: 6692804]
11. Hardy JA, Aust AE. The effect of iron binding on the ability of crocidolite asbestos to catalyze DNA single-strand breaks. Carcinogenesis. 1995; 16:319–325. [PubMed: 7859364]
12. Schapira RM, Ghio AJ, Effros RM, Morrisey J, Dawson CA, Hacker AD. Hydroxyl radicals are formed in the rat lung after asbestos instillation in vivo. Am J Respir Cell Mol Biol. 1994; 10:573–579. [PubMed: 8179922]
13. Mossman BT, Marsh JP, Sesko A, Hill S, Shatos MA, Doherty J, Petruska J, Adler KB, Hemenway D, Mickey R. Inhibition of lung injury, inflammation, and interstitial pulmonary fibrosis by polyethylene glycol-conjugated catalase in a rapid inhalation model of asbestosis. Am Rev Respir Dis. 1990; 141:1266–1271. [PubMed: 2160214]
14. Mossman BT, Surinrut P, Brinton BT, Marsh JP, Heintz NH, Lindau-Shepard B, Shaffer JB. Transfection of a manganese-containing superoxide dismutase gene into hamster tracheal epithelial cells ameliorates asbestos-mediated cytotoxicity. Free Radic Biol Med. 1996; 21:125–131. [PubMed: 8818626]
15. Panduri V, Weitzman SA, Chandel N, Kamp DW. The mitochondria-regulated death pathway mediates asbestos-induced alveolar epithelial cell apoptosis. Am J Respir Cell Mol Biol. 2003; 28:241–248. [PubMed: 12540492]
16. Marklund SL. Extracellular superoxide dismutase and other superoxide dismutase isoenzymes in tissues from nine mammalian species. Biochem J. 1984; 222:649–655. [PubMed: 6487268]
17. Marklund SL. Extracellular superoxide dismutase in human tissues and human cell lines. J Clin Invest. 1984; 74:1398–1403. [PubMed: 6541229]
18. Marklund SL. Human copper-containing superoxide dismutase of high molecular weight. Proc Natl Acad Sci U S A. 1982; 79:7634–7638. [PubMed: 6961438]
19. Fattman CL, Schaefer LM, Oury TD. Extracellular superoxide dismutase in biology and medicine. Free Radic Biol Med. 2003; 35:236–256. [PubMed: 12885586]
20. Cantin AM, North SL, Fells GA, Hubbard RC, Crystal RG. Oxidant-mediated epithelial cell injury in idiopathic pulmonary fibrosis. J Clin Invest. 1987; 79:1665–1673. [PubMed: 3034979]
21. Thannickal VJ, Toews GB, White ES, Lynch JP 3rd, Martinez FJ. Mechanisms of pulmonary fibrosis. Annu Rev Med. 2004; 55:395–417. [PubMed: 14746528]

22. Fattman CL, Chu CT, Kulich SM, Enghild JJ, Oury TD. Altered expression of extracellular superoxide dismutase in mouse lung after bleomycin treatment. Free Radic Biol Med. 2001; 31:1198–1207. [PubMed: 11705698]
23. Tan RJ, Fattman CL, Watkins SC, Oury TD. Redistribution of pulmonary EC-SOD after exposure to asbestos. J Appl Physiol. 2004; 97:2006–2013. [PubMed: 15298984]
24. Tan RJ, Fattman CL, Niehouse LM, Tobolewski JM, Hanford LE, Li Q, Monzon FA, Parks WC, Oury TD. Matrix metalloproteinases promote inflammation and fibrosis in asbestos-induced lung injury in mice. Am J Respir Cell Mol Biol. 2006; 35:289–297. [PubMed: 16574944]
25. Tan RJ, Lee JS, Manni ML, Fattman CL, Tobolewski JM, Zheng M, Kolls JK, Martin TR, Oury TD. Inflammatory cells as a source of airspace extracellular superoxide dismutase after pulmonary injury. Am J Respir Cell Mol Biol. 2006; 34:226–232. [PubMed: 16224105]
26. Fattman CL, Chang LY, Termin TA, Petersen L, Enghild JJ, Oury TD. Enhanced bleomycin-induced pulmonary damage in mice lacking extracellular superoxide dismutase. Free Radic Biol Med. 2003; 35:763–771. [PubMed: 14583340]
27. Fattman CL, Tan RJ, Tobolewski JM, Oury TD. Increased sensitivity to asbestos-induced lung injury in mice lacking extracellular superoxide dismutase. Free Radic Biol Med. 2006; 40:601–607. [PubMed: 16458190]
28. Gao F, Koenitzer JR, Tobolewski JM, Jiang D, Liang J, Noble PW, Oury TD. Extracellular superoxide dismutase inhibits inflammation by preventing oxidative fragmentation of hyaluronan. J Biol Chem. 2008; 283:6058–6066. [PubMed: 18165226]
29. Brass DM, Hoyle GW, Poovey HG, Liu JY, Brody AR. Reduced tumor necrosis factor-alpha and transforming growth factor-beta1 expression in the lungs of inbred mice that fail to develop fibroproliferative lesions consequent to asbestos exposure. Am J Pathol. 1999; 154:853–862. [PubMed: 10079263]
30. Brass DM, Tsai SY, Brody AR. Primary lung fibroblasts from the 129 mouse strain exhibit reduced growth factor responsiveness in vitro. Exp Lung Res. 2001; 27:639–653. [PubMed: 11768716]
31. Warshamana GS, Pociask DA, Sime P, Schwartz DA, Brody AR. Susceptibility to asbestos-induced and transforming growth factor-beta1-induced fibroproliferative lung disease in two strains of mice. Am J Respir Cell Mol Biol. 2002; 27:705–713. [PubMed: 12444030]
32. Pierce A, Whitlark J, Dory L. Extracellular superoxide dismutase polymorphism in mice. Arterioscler Thromb Vasc Biol. 2003; 23:1820–1825. [PubMed: 12893682]
33. Jun S, Pierce A, Dory L. Extracellular superoxide dismutase polymorphism in mice: Allele-specific effects on phenotype. Free Radic Biol Med. 2010; 48:590–596. [PubMed: 20005946]
34. Lowry OH, Rosebrough NJ, Farr AL, Randall RJ. Protein measurement with the folin phenol reagent. J Biol Chem. 1951; 193:265–275. [PubMed: 14907713]
35. Marklund SL. Analysis of extracellular superoxide dismutase in tissue homogenates and extracellular fluids. Methods Enzymol. 1990; 186:260–265. [PubMed: 2233298]
36. Paoletti F, Mocali A. Determination of superoxide dismutase activity by purely chemical system based on NAD(P)H oxidation. Methods Enzymol. 1990; 186:209–220. [PubMed: 2233293]
37. Laemmli UK. Cleavage of structural proteins during the assembly of the head of bacteriophage T4. Nature. 1970; 227:680–685. [PubMed: 5432063]
38. Woessner JF Jr. The determination of hydroxyproline in tissue and protein samples containing small proportions of this imino acid. Arch Biochem Biophys. 1961; 93:440–447. [PubMed: 13786180]
39. Gongora MC, Lob HE, Landmesser U, Guzik TJ, Martin WD, Ozumi K, Wall SM, Wilson DS, Murthy N, Gravanis M, Fukai T, Harrison DG. Loss of extracellular superoxide dismutase leads to acute lung damage in the presence of ambient air: A potential mechanism underlying adult respiratory distress syndrome. Am J Pathol. 2008; 173:915–926. [PubMed: 18787098]
40. Carlsson LM, Jonsson J, Edlund T, Marklund SL. Mice lacking extracellular superoxide dismutase are more sensitive to hyperoxia. Proc Natl Acad Sci U S A. 1995; 92:6264–6268. [PubMed: 7603981]
41. Bowler RP, Nicks M, Tran K, Tanner G, Chang LY, Young SK, Worthen GS. Extracellular superoxide dismutase attenuates lipopolysaccharide-induced neutrophilic inflammation. Am J Respir Cell Mol Biol. 2004; 31:432–439. [PubMed: 15256385]

42. Folz RJ, Abushamaa AM, Suliman HB. Extracellular superoxide dismutase in the airways of transgenic mice reduces inflammation and attenuates lung toxicity following hyperoxia. J Clin Invest. 1999; 103:1055–1066. [PubMed: 10194479]

43. Bowler RP, Nicks M, Warnick K, Crapo JD. Role of extracellular superoxide dismutase in bleomycin-induced pulmonary fibrosis. Am J Physiol Lung Cell Mol Physiol. 2002; 282:L719–26. [PubMed: 11880297]

44. Kliment CR, Englert JM, Gochuico BR, Yu G, Kaminski N, Rosas I, Oury TD. Oxidative stress alters syndecan-1 distribution in lungs with pulmonary fibrosis. J Biol Chem. 2009; 284:3537–3545. [PubMed: 19073610]

45. Kliment CR, Tobolewski JM, Manni ML, Tan RJ, Enghild J, Oury TD. Extracellular superoxide dismutase protects against matrix degradation of heparan sulfate in the lung. Antioxid Redox Signal. 2008; 10:261–268. [PubMed: 17961072]

46. Juul K, Tybjaerg-Hansen A, Marklund S, Lange P, Nordestgaard BG. Genetically increased antioxidative protection and decreased chronic obstructive pulmonary disease. Am J Respir Crit Care Med. 2006; 173:858–864. [PubMed: 16399992]

47. Siedlinski M, van Diemen CC, Postma DS, Vonk JM, Boezen HM. Superoxide dismutases, lung function and bronchial responsiveness in a general population. Eur Respir J. 2009; 33:986–992. [PubMed: 19213780]

48. Yamada H, Yamada Y, Adachi T, Fukatsu A, Sakuma M, Futenma A, Kakumu S. Protective role of extracellular superoxide dismutase in hemodialysis patients. Nephron. 2000; 84:218–223. [PubMed: 10720891]

49. Juul K, Tybjaerg-Hansen A, Marklund S, Heegaard NH, Steffensen R, Sillesen H, Jensen G, Nordestgaard BG. Genetically reduced antioxidative protection and increased ischemic heart disease risk: The Copenhagen city heart study. Circulation. 2004; 109:59–65. [PubMed: 14662715]

50. Tamai M, Furuta H, Kawashima H, Doi A, Hamanishi T, Shimomura H, Sakagashira S, Nishi M, Sasaki H, Sanke T, Nanjo K. Extracellular superoxide dismutase gene polymorphism is associated with insulin resistance and the susceptibility to type 2 diabetes. Diabetes Res Clin Pract. 2006; 71:140–145. [PubMed: 15990193]

51. Young RP, Hopkins R, Black PN, Eddy C, Wu L, Gamble GD, Mills GD, Garrett JE, Eaton TE, Rees MI. Functional variants of antioxidant genes in smokers with COPD and in those with normal lung function. Thorax. 2006; 61:394–399. [PubMed: 16467073]

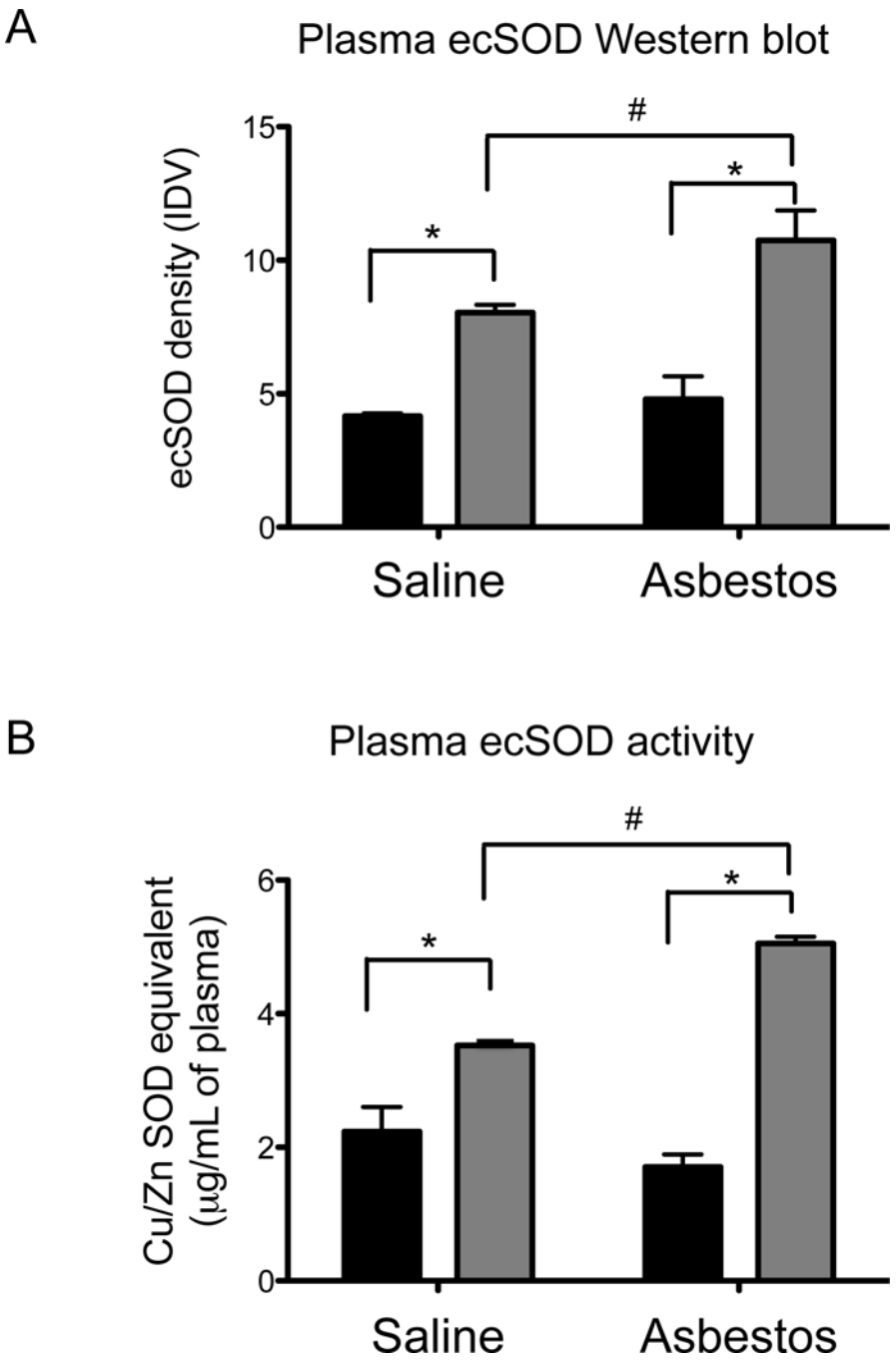

Figure 1. Plasma ecSOD level and activity in saline- and asbestos-treated mice

Plasma ecSOD isolated from control and asbestos-treated *sod3*^{wt} (solid bars) and *sod3*^{129} (grey bars) mice 14 days after treatment (4-5 mice per group). Western blot was performed using an aliquot of plasma (equivalent of 0.5 μL of plasma) and densitometric analysis is shown in A. (B) Activities of plasma ecSOD were measured using a semi-purified sample of plasma by ConA-affinity chromatography.

Error bars represent ±SEM.

* $p < 0.05$ versus *sod3*^{wt} mice;

# $p < 0.05$ versus saline control.

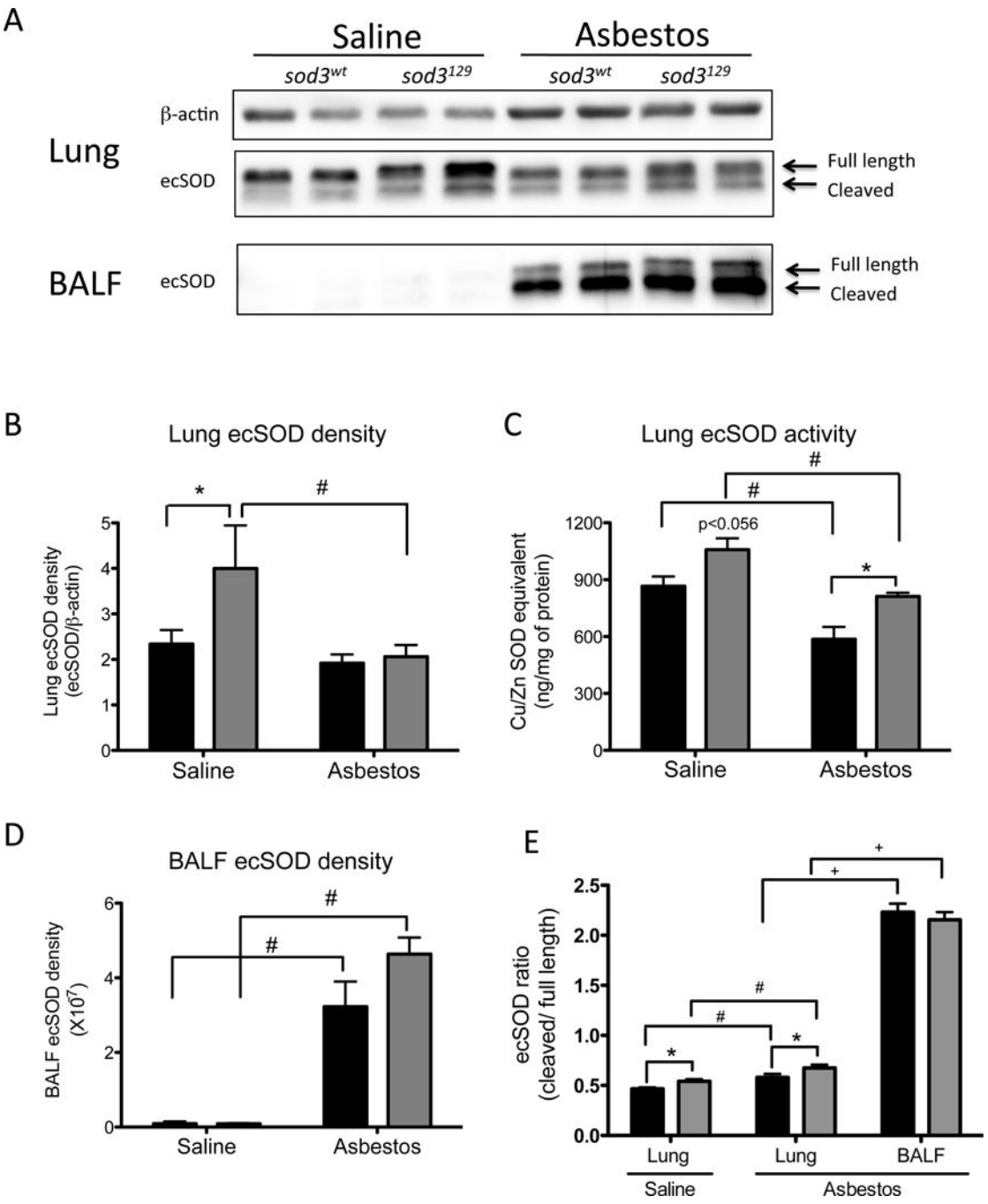

Figure 2. The effect of asbestos treatment on ecSOD in lung tissue and BALF

Lung and BALF ecSOD isolated from saline and asbestos-exposed *sod3*^{129} (grey bars) and *sod3*^{wt} (solid bars) mice 14 days after treatment (5-7 mice per group). Western blot (A) was performed using 10 μg of total lung protein or 20 μL of BALF and densitometric analyses of lung and BALF ecSOD are shown in B and D, respectively. Lung ecSOD densitometry was normalized to β-actin as an internal loading control. (C) Activities of ecSOD from control and asbestos-treated *sod3*^{129} and *sod3*^{wt} mice. ecSOD was isolated from lung homogenates by ConA-affinity chromatography which separates ecSOD from other intracellular SODs.

(E) The ratio of cleaved to full-length forms of ecSOD in lung and BALF. Error bars represent ±SEM.

* $p < 0.05$ versus *sod3*^{wt} mice;

# $p < 0.05$ versus saline control;

+ $p < 0.05$ versus lung.

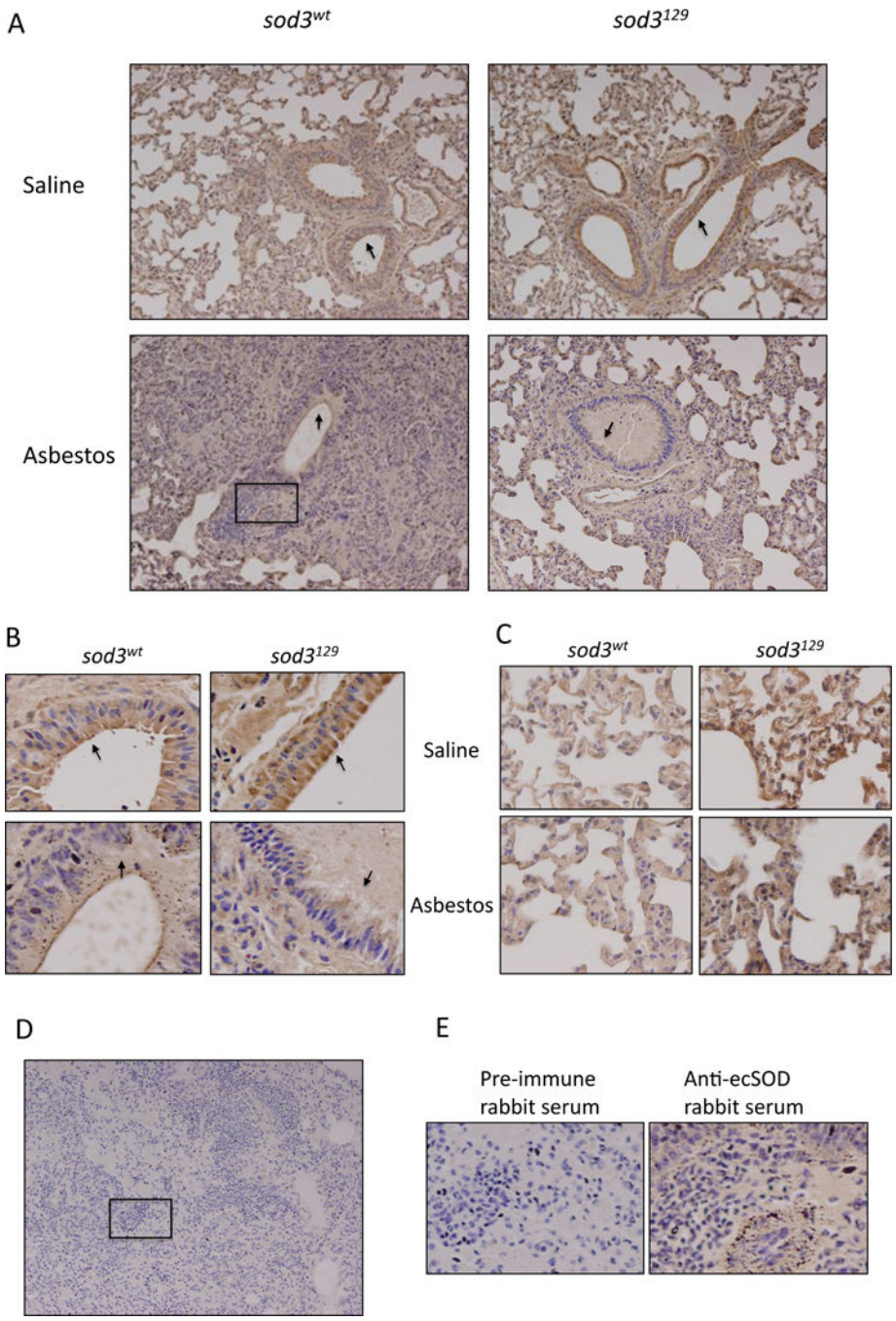

Figure 3. ecSOD localization in saline- and asbestos-treated mice

Immunohistochemical staining for ecSOD (dark brown color) was performed on 5μ-thick sections of lung tissue, obtained from saline- and asbestos-treated mice, as described in Methods. Hematoxylin (blue) was used for counter staining. Typical micrographs (100× mag) are shown (A). The bronchioles are indicated with arrows and the enlarged micrographs of the epithelial lining of the bronchioles are shown in (B). Staining with non-immune primary antiserum of a section of lung from asbestos-treated *sod3*^{wt} lung is shown

in (C). Enlarged areas of cellular infiltration [outlined by a rectangles in (A) and (C)] are shown in (D).

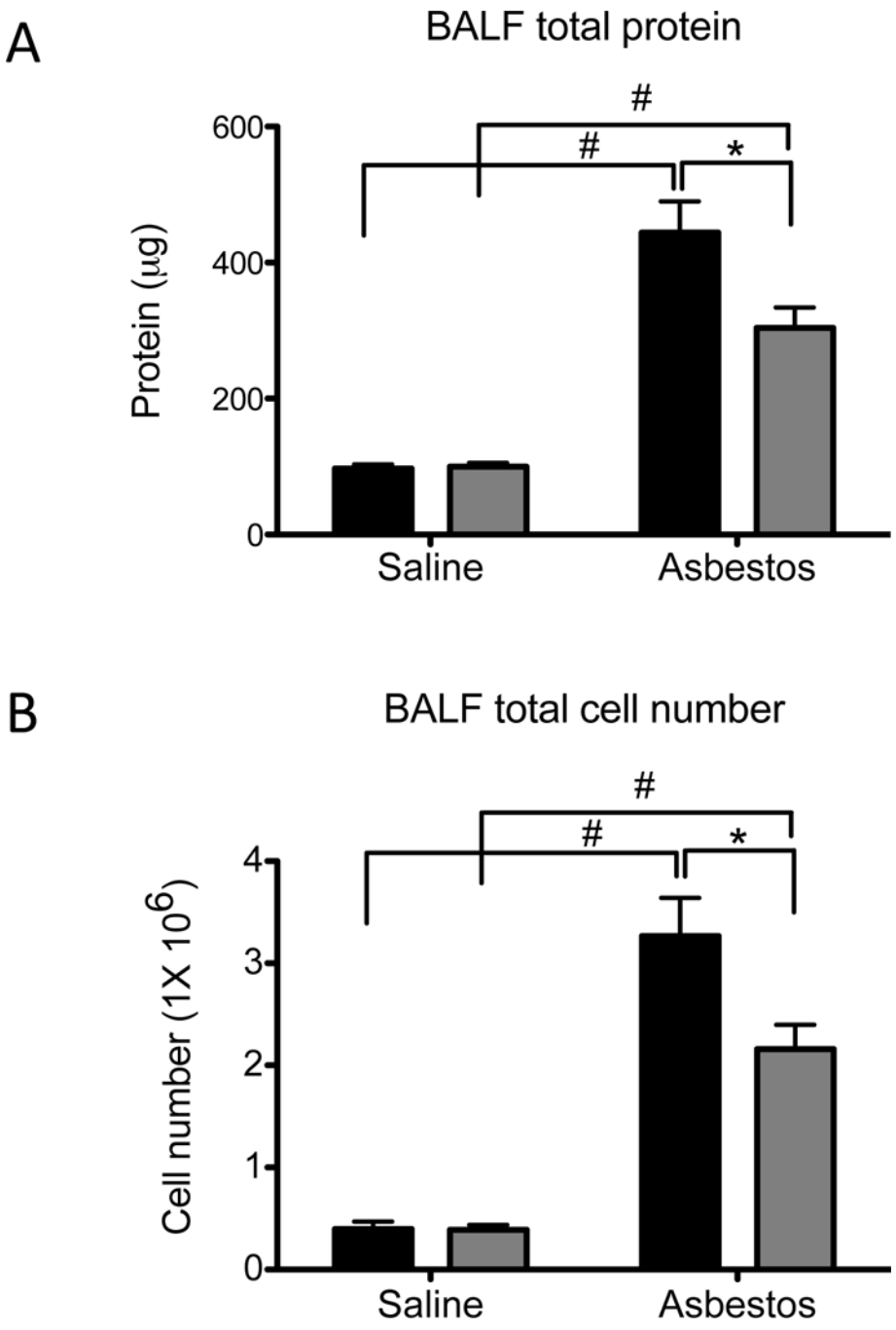

Figure 4. Total protein (A) and cell content (B) of BALF isolated from saline and asbestos-treated mice

Total protein content (A) and cell content (B) in BALF isolated from saline- and asbestos-treated *sod3*^{129} (grey bars) and *sod3*^{wt} (solid bars) mice (5-7 mice per group). Error bars represent ±SEM.

* $p < 0.05$ versus *sod3*^{wt} mice;

# $p < 0.05$ versus saline control.

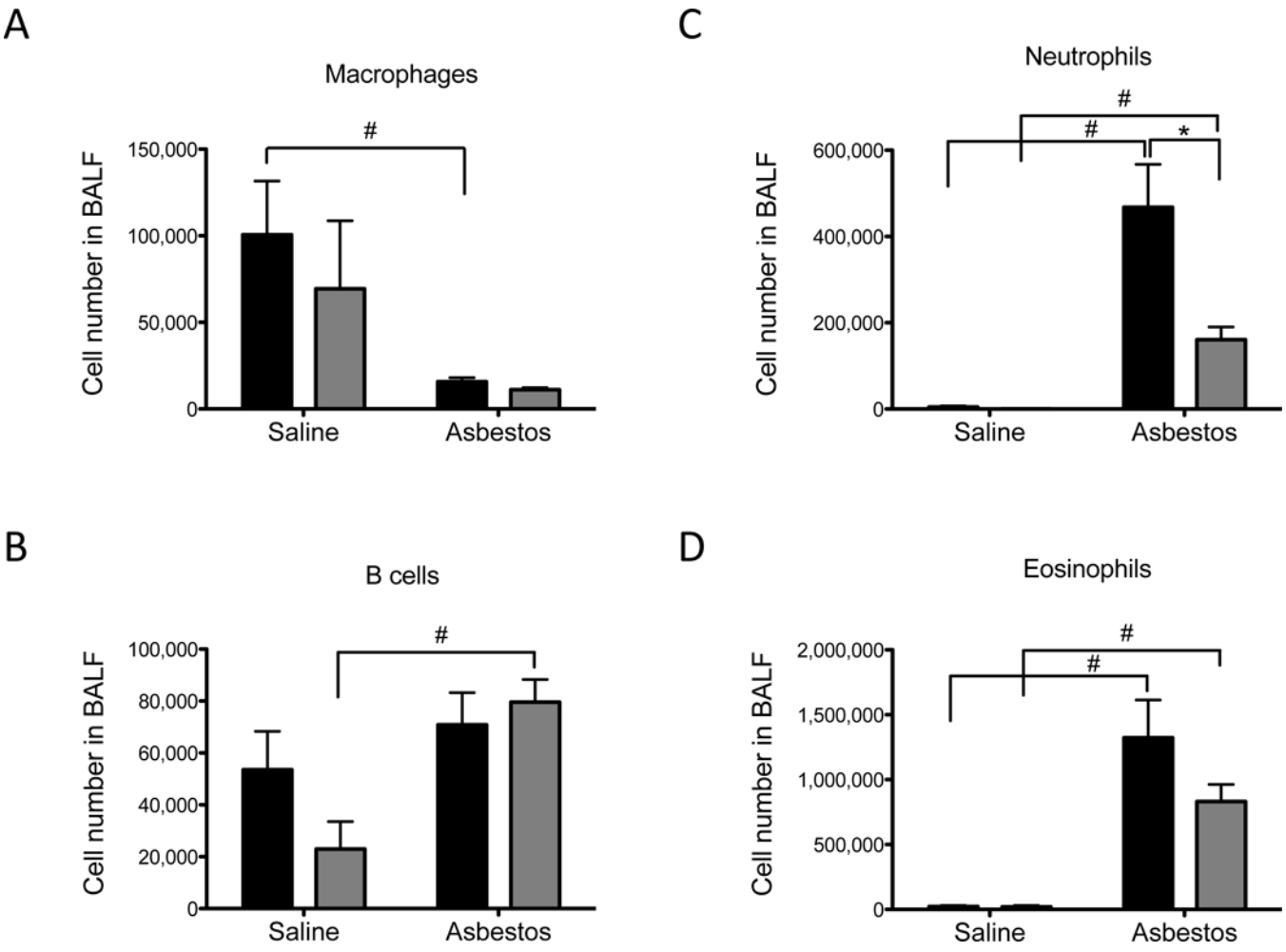

Figure 5. Analysis of BALF cell content by flow cytometry

Macrophages (A), B cells (B), neutrophils (C) and eosinophils (D) in BALF isolated from saline- and asbestos-treated *sod3*^{129} (grey bars) and *sod3*^{wt} (solid bars) mice (5-7 mice per group). Cell specific markers were used to differentiate each cell types: F4/80(+) for macrophages; B220(+) for B cells; Ly6G(+)/CD11b(+) for neutrophils; SiglecF(+)/ CD11b(+) for eosinophils. Error bars represent ±SEM.

* $p < 0.05$ versus *sod3*^{wt} mice;

# $p < 0.05$ versus saline control.

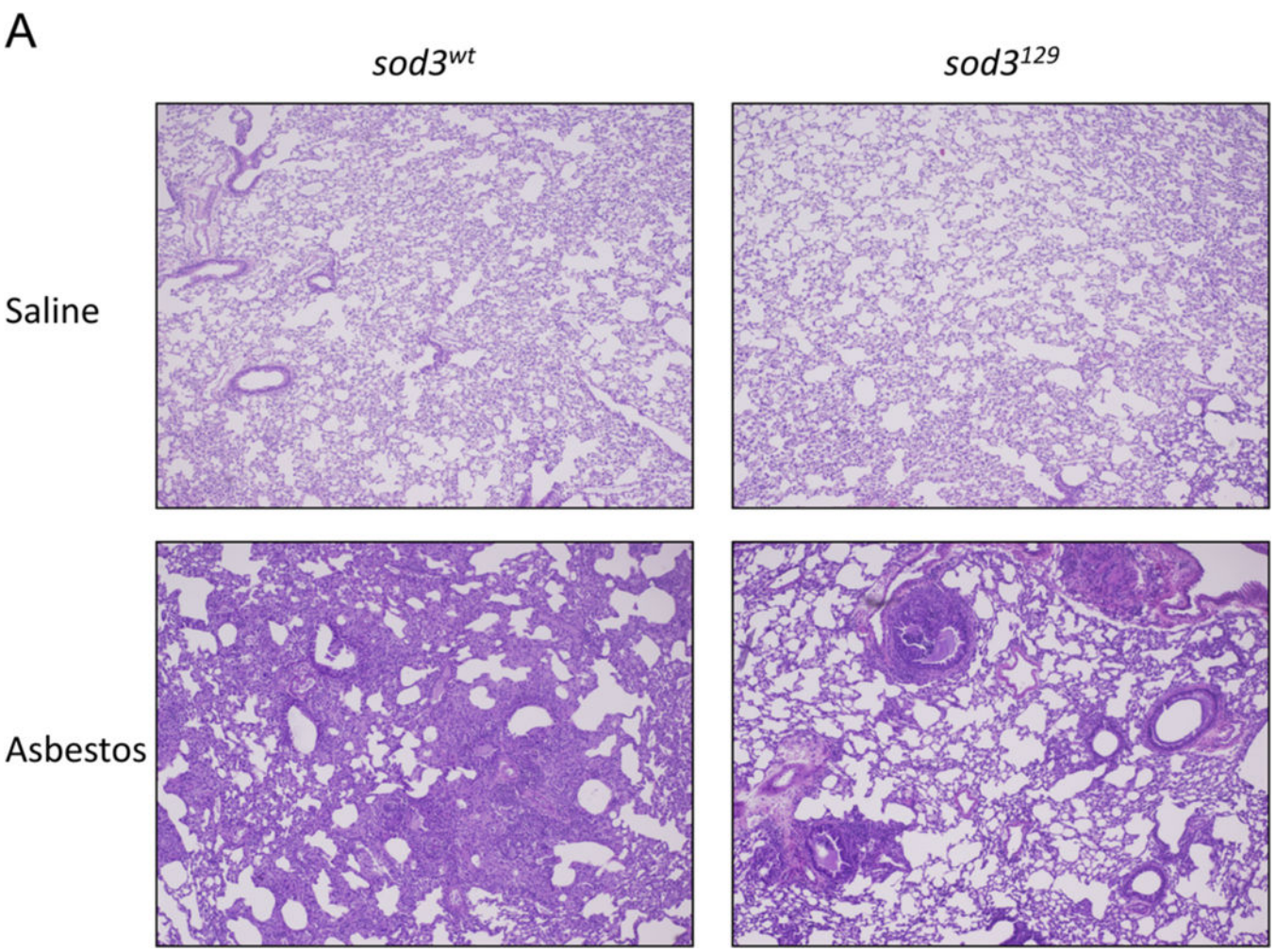

Figure 6. H & E staining and typical micrographs (A), pathology indices (B) and hydroxyproline content of lung tissues isolated from saline- or asbestos-treated mice

Hematoxylin and eosin (H & E) staining was performed on 5 μ thick sections of lung tissue, obtained from saline- and asbestos-treated mice, as described in Methods. Typical micrographs (40× mag) are shown in (A). Mean pathology index scores (B) of lung tissue sections were determined, as described in Methods. The extent of collagen deposition, as measured by hydroxyproline content of lung tissue is shown in (C). Lung tissue from saline- and asbestos-treated *sod3*^{129} (grey bars) *and sod3*^{wt} (solid bars) was used (5-7 mice per group). Error bars represent ±SEM.

* $p < 0.05$ versus *sod3*^{wt} mice;

# $p < 0.05$ versus saline control.